Classical Atomic Form Factor

D. Vrinceanu and M. R. Flannery
School of Physics, Georgia Institute of Technology, Atlanta, Georgia 30332
(Received 25 November 1998)

The general trends exhibited in the variation of the inelastic form factor in collisional transitions $nl \to n'l'$, when l' is changed and n, l, and n' are kept fixed, are explained solely in terms of classical mechanics. Previous quantal results are reproduced from purely classical mechanics principles. Our conclusions are valid not only for large quantum numbers (which provide the usual classical correspondence) but also for other cases, which, up to now have been described only by quantal or semiclassical methods. The interesting trends exhibited in the form factor are directly reflected in experimental and theoretical treatments of collisions involving excited atoms. [S0031-9007(99)09037-7]

PACS numbers: 32.80.Cy, 31.15.Gy, 34.50.–s

With the advent of new technology which facilitates the accurate measurement [1] of electron-excited atom collision cross section there has also been renewed interest in the theory [2] of collisions involving Rydberg atoms. Recent experiment [1], in particular, has confirmed that the cross section for the quadrupole $2^3S \to 3^3D$ transition in $e - \mathrm{He}(2^3S)$ collisions is much higher than that for the pure dipole $2^3S \to 3^3P$ transition at low and intermediate energies, in accord with the theoretical predictions of Ref. [3] (Born and multichannel eikonal approximations). Flannery and McCann [4] have noted that this unexpected behavior is only part of a more general systematic trend in that (a) the $2^3S \to n^3D$ collisional transitions are predominant over all other transitions to the same n value, even for transitions to the electronic continuum, and (b) there is a unique value $l'_{\max}$ of the final angular momentum l' that is preferentially populated in $nl \to n'l'$ transitions ($n' \gg n$) in collisions between Rydberg atoms and electrons or atoms.

The origin of this general behavior was traced [4] to the variation with l' of the quantum mechanical inelastic form factor

$$\mathcal{F}_{fi}(\mathbf{q}) = \langle \psi_f(\mathbf{r}) | e^{i\mathbf{q}\mathbf{r}/\hbar} | \psi_i(\mathbf{r}) \rangle = \langle \phi_f(\mathbf{p} + \mathbf{q}) | \phi_i(\mathbf{p}) \rangle \tag{1}$$

for $i(n,l) \to f(n',l')$ transitions between atomic states; $\psi_{i,f}(\mathbf{r})$ are the wave functions in position space and $\phi_{i,f}(\mathbf{p}) = (2\pi\hbar)^{-3/2} \int \psi_{i,f}(\mathbf{r}) \exp(-i\mathbf{p}\mathbf{r}/\hbar)\, d\mathbf{r}$, the wave functions in momentum space.

When an instantaneous impulse applied at $t = t_0$ transfers momentum $\mathbf{q}$ to an atomic electron, the exact solution of Schrödinger's equation under Hamiltonian

$$H(\mathbf{p},\mathbf{r},t) = \mathbf{p}^2/2m - e^2/r - \mathbf{r}\cdot\mathbf{q}\,\delta(t - t_0) \tag{2}$$

is

$$\Psi(\mathbf{r},t) = [1 + (e^{i\mathbf{q}\mathbf{r}/\hbar} - 1)\theta(t - t_0)]\psi_{nlm}(\mathbf{r}),$$

where θ is the Heaviside step function. The probability for $i \equiv |nl\rangle \to f \equiv |n'l'\rangle$ transitions from the $(2l + 1)$ initial sublevels is then

$$P_{nl,n'l'}(q) = |\langle \psi_{n'l'} | \Psi \rangle|^2 = \sum_{m,m'} |\langle n'l'm' | e^{i\mathbf{q}\cdot\mathbf{r}/\hbar} | nlm \rangle|^2 \tag{3}$$

also deduced in [5]. The probability of any impulsive $i \to f$ transition, whether due to particle collisions or electromagnetic field, is therefore

$$P_{if}(\mathbf{q}) = |\mathcal{F}_{fi}(\mathbf{q})|^2, \tag{4}$$

which provides physical significance to the inelastic form factor, a fundamental property of the atom. For impulsive collisions between a particle 1 and a Rydberg electron 2 bound to a core 3, the overall transition matrix element T decomposes as [5]

$$T_{if}(\mathbf{q}) = \mathcal{F}_{fi}(\mathbf{q}) T_{12}(\mathbf{q}), \tag{5}$$

where T_{12}, the matrix element for (1-2) free-free elastic scattering in the (1-2) center of mass, is a function only of $\mathbf{q}$, as for Coulomb scattering $T_{12} = 4\pi\hbar^2 e^2/q^2$, or for Born's approximation, $T_{12} = \int V(\mathbf{r}_{12}) \exp(i\mathbf{q}\mathbf{r}/\hbar)\, d\mathbf{r}_{12}$. The probability of transition in the target atom per each (1-2) impulsive encounter is $P_{if} = |T_{if}|^2/|T_{12}|^2$, in agreement with (4).

The cross section is obtained by the following integration of the form factor (5) over momentum change,

$$\sigma_{if} = \left(\frac{2\pi}{M_{12}^2 v_i^2}\right) \int_{|k_i - k_f|}^{k_i + k_f} |\mathcal{F}_{fi}(q)|^2\, |f_{12}(q)|^2\, q\, dq, \tag{6}$$

where $k_{i,f}$ are the initial and final wave numbers of relative motion of the projectile-target system of reduced mass M and $q = \hbar|\mathbf{k}_i - \mathbf{k}_f|$ is the momentum change. The scattering amplitude for (1-2) collisions of reduced mass M_{12} is $f_{12} = (2M_{12}/4\pi\hbar^2)T_{12}$. For (1-2) slow collisions with scattering length a, the Fermi interaction $V(\mathbf{r}_{12}) = [4\pi a(\hbar^2/M_{12})]\delta(\mathbf{r}_1 - \mathbf{r}_2)$ also yields decomposition (5) with $f_{12} = a$.

The inelastic quantal form factor therefore not only exerts primary importance in collision studies, but also has a deep physical reality. In recent experimental studies

 0031-9007/99/82(17)/3412(4)$15.00

of excitation of Rydberg atoms by short unipolar half-cycle electromagnetic pulses the transition amplitude is determined directly by the inelastic form factor [6].

Analytical quantal [7,8] and semiclassical [9] form factors are available, although general systematic trends cannot be easily extracted from them. A classical form factor for $n \to n'$ has been deduced [10] from binary encounter impulse theory and from a microcanonical distribution in energy space. A key point of this paper is that a complementary classical approach for $nl \to n'l'$ transitions can also be developed in a way which reveals, quite succinctly, important aspects which remain hidden within the quantal treatment.

Consider a Rydberg atom in a stationary (n, l) state with energy E and angular momentum L. If the atom is perturbed by any general impulsive field [as in Eq. (2) or the Fermi interaction], then the transition probability to the final state (n', l') (of energy E' and angular momentum L') is the inelastic form factor.

The quantal probability density for finding the electron in the radial interval $(r, r + dr)$ is

$$\rho^q_{nl}(r) = r^2 |R_{nl}|^2, \tag{7}$$

where R_{nl} is the hydrogenic radial wave function expressed in terms of the generalized Laguerre polynomial.

The phase space of a classical atom, with Hamiltonian $H(\mathbf{r}, \mathbf{p}) = p^2/2m + V(r)$, angular momentum $\mathbf{L}(\mathbf{r}, \mathbf{p}) = \mathbf{r} \times \mathbf{p}$, and period $\tau_{nl} = \nu^{-1}_{nl}$ in stationary state (n, l) is populated according to the microcanonical distribution [8,10]

$$\rho^c_{nl}\, d\mathbf{r}\, d\mathbf{p} = \{h\nu_{nl}\hbar\delta(H - E)\delta(|\mathbf{L}| - L)\}\, \frac{d\mathbf{r}\, d\mathbf{p}}{(2\pi\hbar)^3} \tag{8}$$

normalized to $(2l + 1)$ states in all of phase space. On integrating over the momentum space $\mathbf{p}$ and angular part $\hat{r}$ of the configuration space $\mathbf{r}$, the classical distribution is

$$\rho^c_{nl}(r)\, dr = \frac{2l + 1}{\tau_{nl}}\, \frac{2}{\dot{r}}\, dr\,,$$

where the radial speed is given by $m\dot{r}^2/2 = E - V(r) - (l + 1/2)^2\hbar^2/2mr^2$. For the Kepler atom ($\tau_{nl} = 2\pi n^3$ a.u.) and ρ^c_{nl} (in a.u.) is

$$\rho^c_{nl}(r) = \frac{1}{\pi n^3}\left[\frac{2}{r} - \frac{1}{n^2} - \frac{(l + 1/2)^2}{r^2}\right]^{-1/2} = \frac{1}{\pi n^3}\,\frac{1}{\dot{r}(r)}\,. \tag{9}$$

The quantal (7) and classical (9) radial probability densities are illustrated in Fig. 1. As in the textbook example of the harmonic oscillator, the classical distribution has singularities at the corresponding turning points given by the radii (in a.u.)

$$R^{\pm} = n^2\{1 \pm \epsilon\} = n^2\{1 \pm [1 - (l + 1/2)^2/n^2]^{1/2}\}. \tag{10}$$

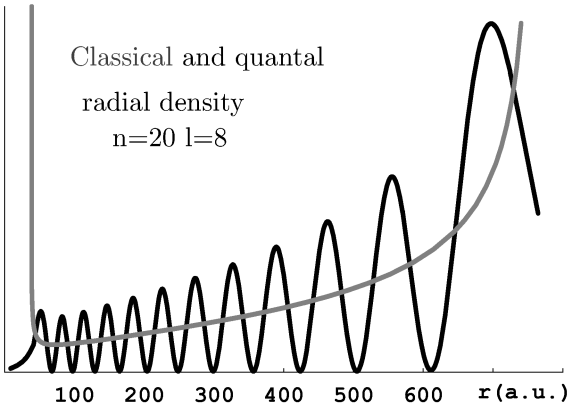

FIG. 1. Classical and quantal radial densities of probability of localization for the stationary state of the hydrogen atom [$E = -1/(2 \times 20^2)$ and $l = 8$].

The classical distribution is zero outside the accessible region, bounded by $R^{\pm}$.

By using definition (1) the transition probability (3) can be converted to the new form

$$P_{if}(\mathbf{q}) = (2\pi\hbar)^3 \int \rho_{nl}(\mathbf{r}, \mathbf{p})\rho^*_{n'l'}(\mathbf{r}, \mathbf{p} + \mathbf{q})\, d\mathbf{r}\, d\mathbf{p}\,, \tag{11}$$

where the quantal distributions in phase space are given by $\rho^q(\mathbf{r}, \mathbf{p}) = (2\pi\hbar)^{-3/2}\psi(\mathbf{r}) \exp(-i\mathbf{p} \cdot \mathbf{r}/\hbar)\phi^*(\mathbf{p})$. This form is now suitable for classical correspondence obtained by replacing densities ρ^q by the phase space distributions (8). The basic definition of the classical form factor is therefore given by (8) and (11). The physical significance is that the initial and final states correspond to definite regions in phase space, populated according to the microcanonical distribution (8), and that the transition probability is given, in a geometric sense, by the amount of overlap of these regions. In configuration space alone, the regions are spherical shells with inner and outer radii given by Eq. (10), the pericenter (R^-) and apocenter (R^+) of the Kepler orbit.

Analytical expressions with explicit dependence on $\mathbf{q}$ for quantal and classical probabilities for $nl \to n'l'$, $nl \to n'$, $n \to n$ transitions are developed in a separate paper [8]. Rather than examining the l' variation of (11) for a given q, the key results are more readily deduced and are easily transparent by investigating the probability for all momentum transfers

$$F^c_{nl\to n'l'} = \int P_{if}(\mathbf{q})\, d\mathbf{q} = (2\pi\hbar)^3 \int_{\mathcal{R}} d\mathbf{r}\, \rho^c_{nl}(\mathbf{r})\rho^c_{n'l'}(\mathbf{r})\,, \tag{12}$$

where $\mathcal{R}$ is the overlapping region in configuration space defined by intersection of (R^-_i, R^+_i) and (R^-_f, R^+_f) intervals.

Inserting $\rho(\mathbf{r}) = 4\pi\rho^c(r)r^2$ with (9) in (12) gives the classical form factor (CFF)

$$F^c_{nl\to n'l'} = 2\,\frac{(2l'+1)}{n^3 n'^3}\int_{R_{\min}}^{R_{\max}} \frac{dr/r^2}{\dot{r}_i(r)\dot{r}_f(r)}, \qquad (13)$$

where $R_{\min} = \max(R_i^-, R_f^-)$ and $R_{\max} = \min(R_i^+, R_f^+)$ define the bounds of the overlapping region $\mathcal{R}$. Different overlap situations are illustrated in Fig. 2 for a representative case. The gray region is the accessible region for the initial state and the curves are possible final state trajectories. Transitions occur only when the final state trajectory penetrates the initial state accessible region. The longer time spent by the electron on the final state trajectory within the initial state accessible region, the bigger is the transition probability.

As l increases from zero to its maximum value for circular orbits, R^- increases from zero to n^2, while R^+ decreases from $2n^2$ to the same value n^2. For final states $n' > \sqrt{2}\,n$, then $R_{\max} = R_i^+$ for all values of l'. Three regions of overlap are then apparent and are, respectively, accessed as l' is increased.

Region I, $R_f^- < R_i^-$.—Here the overlap region $\mathcal{R} \equiv (R_i^-, R_i^+)$ is determined solely by the initial state and has spatial extent which remains constant as l' is varied from zero to some value l_1 where $R_f^- = R_i^-$. There is always an orientation of the final orbit which will then intersect the initial orbit, as exhibited in Fig. 2, for $(n = 3,\ l = 2)$ and $(n' = 8,\ l' = 0 - 2)$ orbits. The l' variation of (13) is contained solely within the increasing integrand $(\dot{r}_f)^{-1}$.

Region II, $R_i^- < R_f^-$.—Here the overlap region $\mathcal{R} \equiv (R_f^-,\ R_i^+)$ includes the f pericenter and has spatial extent which decreases, as l' increases, eventually to zero when $R_f^- = R_i^+$. In this region, the initial and final orbits can intersect each other, as for the $(n' = 8,\ l' = 4)$ orbit in Fig. 2. The l' variation of (13) results from variation of both the increasing lower limit R_f^- and the increasing integrand $(\dot{r}_f)^{-1}$.

Region III, $R_f^- > R_i^+$.—Here the initial and final trajectories no longer intersect, since the pericenter of the final state is greater than the apocenter of the initial state. This region where $(i \to f)$ transitions do not occur, as illustrated by $(n' = 8,\ l' = 5, 6, 7)$ orbits in Fig. 2, is the classically inaccessible region.

The boundaries between regions I and II and between regions II and III occur, respectively, at $l' = l_1$ where $R_f^-(n', l') = R_i^-(n, l)$ and at $l' = l_2$ where $R_f^-(n', l') = R_i^+(n, l)$. Thus l_1 and l_2 are given by

$$\left(l_{1,2} + \frac{1}{2}\right)^2 = n^2(1 \mp \varepsilon)[2 - (1 \mp \varepsilon)n^2/n'^2], \qquad (14)$$

where ϵ is the eccentricity $[1 - (l + 1/2)^2/n^2]^{1/2}$ of the initial orbit.

Variation of the CFF (13), with final angular momentum l' is then determined both by the lower integration limit $R_{\min}$ (which is a constant R_i^- in region I and increases as R_f^- in region II) and by the integrand $(\dot{r}_f)^{-1}$. Figure 3 illustrates the general pattern. As l' is increased from 0 to l_1 (region I), the increase in CFF originates purely from the increasing integrand $(\dot{r}_f)^{-1}$. As l' is varied from l_1 to l_2, the increasing integrand is offset by the decreasing range (R_f^-, R_i^+) of integration (region II). For $l_2 < l' < n - 1$, CFF is zero because transitions are not classically allowed in region III.

At $l' = l_1$ the trajectories touch only at their corresponding pericenters and CFF has a turning point singularity characteristic of classical descriptions. The zero radial speed of the electron at the contact point of both initial and final orbits causes the infinite CFF (transition probability).

As is evident from Figs. 3–5, the agreement between the classical and quantal results is excellent in region I, even for small quantum numbers. In region II, the quantal results oscillate about CFF. Since classical motion is confined to a definite region, the dramatic fall for large l' is steeper than that for the quantal case where states

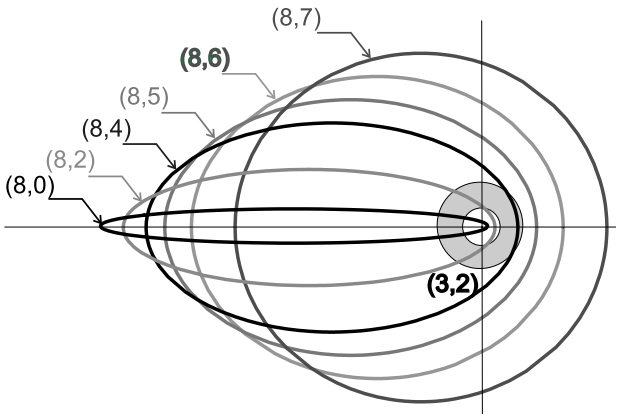

FIG. 2. Various final state $(n' = 8,\ l' = 1{-}7)$ trajectories and the initial accessible region corresponding to $(n = 3,\ l = 2)$.

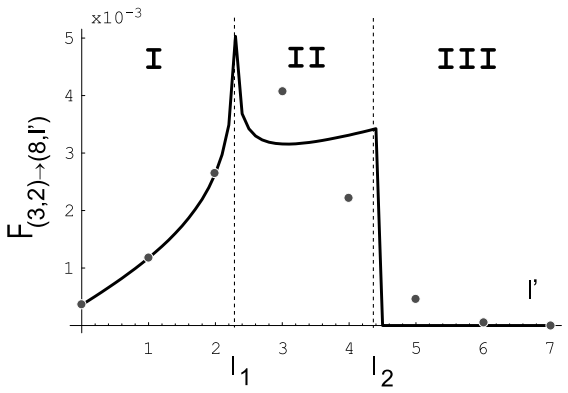

FIG. 3. Characteristic dependence of the inelastic form factor on the final angular momentum l', for fixed n (= 3), l (= 2), and n' (= 8). Classical calculations: solid line; quantal results: dots.

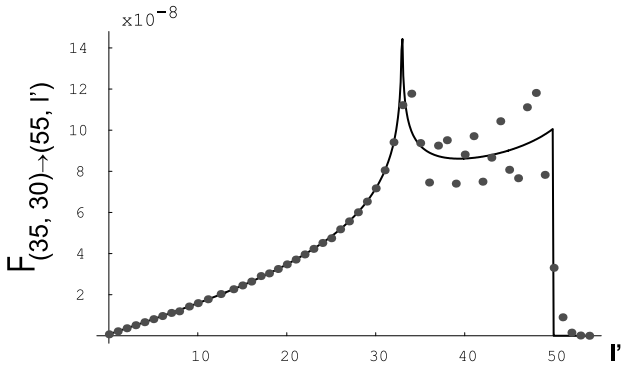

FIG. 4. Classical (solid line) and quantal (dots) inelastic form factor for transitions from state ($n = 35$, $l = 30$) to ($n' = 55$, $l' = 0 \rightarrow 54$) states.

have exponential tails within the classical inaccessible region III. As expected from correspondence principles, for the larger quantum numbers, the quantum form factor tends to CFF, even in the regions II and III, as shown in Fig. 4. For quasielastic transitions $nl \rightarrow nl'$ the classical and quantal results are in excellent agreement for all angular momenta (Fig. 5). The quantal results exhibit maxima in the neighborhood of $l' = l_1, l_2$ where CFF has the classical singularities. The position of l_1 defined by (14) in the limit of large l, where the eccentricity $\varepsilon \rightarrow 0$, is $l_1(l \rightarrow n - 1) = n\sqrt{2}[1 - 1/2(n/n')^2]^{1/2} - 1/2$, an exquisite result for initial circular orbits. For $n' \gg n$, l_1 tends from the bottom to $l_1(l \rightarrow n - 1, n' \gg n) = n\sqrt{2} - 1/2$, a key result in detailed agreement with that previously derived from consideration of the quantal momentum-space overlap [4].

For small initial angular momentum l, $\epsilon \rightarrow 1$ and l_1 is then zero so that the maximum CFF is given by $l_2(l \rightarrow 0) = 2n[1 - (n/n')^2]^{1/2} - 1/2$, appropriate to highly eccentric initial orbits. In the $n' \gg n$ limit then $l_2(l \rightarrow 0, n' \gg n) = 2n - 1/2$. As the initial l increases, there is therefore a slow variation ($2n \rightarrow \sqrt{2}\,n$) in the position l_2 of the maximum of CFF, which is pushed slightly to lower values. This theoretical prediction is also confirmed by the quantal results [4].

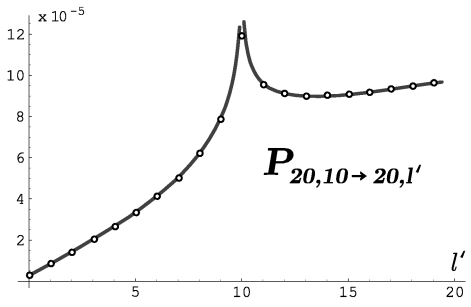

FIG. 5. Classical (solid line) and quantal (dots) inelastic form factor for quasielastic transitions from $n = 20$, $l = 10$ state.

When the energy E' of the final orbit is not sufficient to accommodate the value of l_2 deduced above ($n' < \sqrt{2}\,n$), the peak in CFF (as in Fig. 5) is given by l_1, provided the initial l is large enough. When the final n' is sufficiently small so that the lower l_1 cannot be accommodated, i.e., $l_1 > n' - 1$, CFF and the quantal result exhibit a monotonic increase confined to region I, which is always characterized by excellent agreement between quantal and classical results.

In summary, the pattern exhibited by the l' variations (Figs. 3–5) is essentially identical with the quantal pattern. The positions of maxima of the l' variation of CFF depend strongly on the initial n and only weakly on the initial l, in agreement with the quantal calculations [4], which were restricted to certain cases. Excellent quantitative agreement between classical and quantal results makes the classical form factor a very useful tool particularly at large quantum numbers (Rydberg atoms) where exact quantal results are not easy to obtain (either analytically or numerically) and to use, due to the highly oscillatory nature of the wave function. Although the emphasis here is on the electron form factors, the present analysis is applicable also to form factors for transitions between rovibrational states of molecules.

This work was supported by AFOSR Grant No. F 49620-96-1-0142 and NSF Grant No. 98-02622. One of us (D. V.) thanks Motorola and Gil Amelio for support.

[1] A. R. Filipelli, C. C. Lin, L. W. Anderson, and J. W. McConkey, Adv. At. Mol. Opt. Phys. **33**, 1 (1994); M. E. Lagus, J. B. Boffard, L. W. Anderson, and C. C. Lin, Phys. Rev. A **53**, 1505 (1996).
[2] V. S. Lebedev and I. I. Fabrikant, Phys. Rev. A **54**, 2888 (1996); M. I. Syrkin, Phys. Rev. A **53**, 825 (1996); V. S. Lebedev and V. S. Marchenko, Sov. Phys. JETP **64**, 251 (1986).
[3] M. R. Flannery and K. J. McCann, Phys. Rev. A **12**, 846 (1975).
[4] M. R. Flannery and K. J. McCann, J. Phys. B **12**, 427 (1979); Astrophys. J. **236**, 300 (1980).
[5] M. R. Flannery, Phys. Rev. A **22**, 2408 (1980).
[6] C. O. Reinhold, J. Burgdörfer, R. R. Jones, C. Raman, and P. H. Bucksbaum, J. Phys. B **28**, L457 (1995).
[7] I. Bersons and A. Kulsh, Phys. Rev. A **55**, 1674 (1997).
[8] D. Vrinceanu and M. R. Flannery (to be published).
[9] F. Gounand and L. Petitjean, Phys. Rev. A **30**, 61 (1984).
[10] L. Vriens, *Case Studies in Atomic Collision Physics I*, edited by E. W. McDaniel and M. R. C. McDowell (North-Holland, Amsterdam, 1969), p. 364; V. Borodin, A. K. Kazanski, and V. I. Ochkur, J. Phys. B **25**, 445 (1992).